

# A phosphoramidite-based [FeFe]H<sub>2</sub>ase functional mimic displaying fast electrocatalytic proton reduction†

Sofia Derossi,<sup>‡a</sup> René Becker,<sup>‡a</sup> Ping Li,<sup>a</sup> František Hartl<sup>\*a,b</sup> and Joost N. H. Reek<sup>\*a</sup>

A phosphoramidite modified [FeFe]H<sub>2</sub>ase mimic is studied as a model for photodriven production of H<sub>2</sub>. On cathodic activation, the pyridyl–phosphoramidite complex exhibits a strongly enhanced rate of proton reduction over the previously reported pyridylphosphine model at the same overpotential. Analysis of the cyclic voltammograms shows an apparent H<sub>2</sub> evolution rate strongly influenced by the presence of both side-bound pyridyl and phosphorous-bound dimethylamino moieties at the phosphoramidite ligands. This difference is ascribed to the basic amines acting as proton relays.

Cite this: *Dalton Trans.*, 2014, **43**, 8363

Received 10th December 2013,  
Accepted 3rd April 2014

DOI: 10.1039/c3dt53471e

www.rsc.org/dalton

Efficient photochemical generation of molecular hydrogen is one of the key technologies our society needs in order to move to a sustainable hydrogen-based economy.<sup>1</sup> As a consequence, a great deal of attention has been devoted to (photo-redox)-catalysts performing proton reduction, and both homogeneous and heterogeneous systems have been developed.<sup>2</sup> [FeFe] hydrogenases ([FeFe]H<sub>2</sub>ase) are natural-occurring enzymes that catalyse reduction of protons in an extremely efficient way (TOF ~ 9000 s<sup>-1</sup>).<sup>3</sup> Models of their bimetallic core based on cheap and abundant materials are easily synthesised, which has led to a plethora of diiron mimics.<sup>4</sup> So far, the majority of studies of such bioinspired systems have focused on electrocatalysis,<sup>5</sup> while the direct photodriven catalysis, using a light-harvesting chromophore coupled to the [FeFe] core, has only recently been addressed.<sup>6,7</sup>

The few initial attempts to assess light-driven H<sub>2</sub> production with homogeneous systems are roughly based on four approaches: (i) simple mixing of the chromophore with the catalyst in solution, (ii) electron-transfer mediation by addition of an electron relay in donor–mediator–catalyst systems, (iii) covalent attachment of the chromophore to the catalyst or (iv) supramolecular coordination of the catalyst to the chromophore.<sup>7</sup> The first two strategies offer ease of screening but limit the control over the spatial arrangement between the moieties.

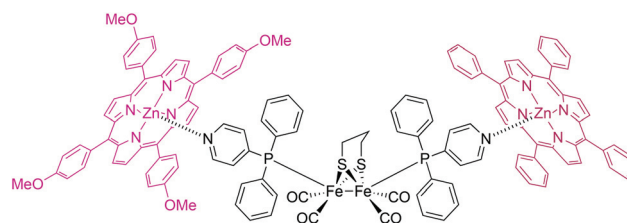


Fig. 1 The active [FeFe]H<sub>2</sub>ase biomimetic supramolecular assembly formed under photoreductive conditions from complex 1 in the presence of two different porphyrins.

However, advantages of a well-defined system in the covalent case come at the price of tedious syntheses and more rapid charge recombination.

We envisaged a supramolecular approach combining the chromophore with the precatalyst to be most advantageous. With this philosophy in mind, we recently introduced 1-ZnTPP, a supramolecular dyad which (after disproportionation into a disubstituted complex, Fig. 1) is capable of a photocatalytic conversion of protons into H<sub>2</sub>.<sup>7</sup> In that case, ZnTPP was chosen as the photosensitizer, while the catalytic mimic 1 was the [Fe<sub>2</sub>(μ-pdt)(CO)<sub>5</sub>L] precursor (Fig. 2). L represents the template ligand<sup>8</sup> *pPyPPH*<sub>2</sub> (*pPy* = 4-pyridyl), which is coordinated to the diiron centre *via* the phosphorus atom and to ZnTPP *via* the *pPy* group (Fig. 1). Under photocatalytic conditions, *i.e.* upon irradiation in the presence of a sacrificial proton- and electron donor, the supramolecular assembly 1-ZnTPP exhibits H<sub>2</sub> evolution, whereas the reference complex (3; L = PPh<sub>3</sub>) is inactive.

Herein, we report development of our supramolecular dyad approach, using *mPyPA*, a recently reported phosphoramidite template ligand based on the binol motif and decorated with two pyridyl groups (Fig. 2, complex 2).<sup>9</sup> We have been intrigued

<sup>a</sup>Van't Hoff Institute for Molecular Sciences, University of Amsterdam, Science Park 904, 1098 XH, Amsterdam, The Netherlands. E-mail: j.n.h.reek@uva.nl; Fax: (+31)205255604; Tel: (+31)205255265

<sup>b</sup>Department of Chemistry, University of Reading, Whiteknights, Reading RG6 6AD, UK. E-mail: f.hartl@reading.ac.uk; Fax: +44 (0)1183786331; Tel: +44 (0)1183786795

† Electronic supplementary information (ESI) available: Syntheses and characterisation of complexes 2 and 4; detailed description of experiments, Fig. S1–S17 and Tables S1–S2. See DOI: 10.1039/c3dt53471e

‡ Both authors contributed equally to this work.



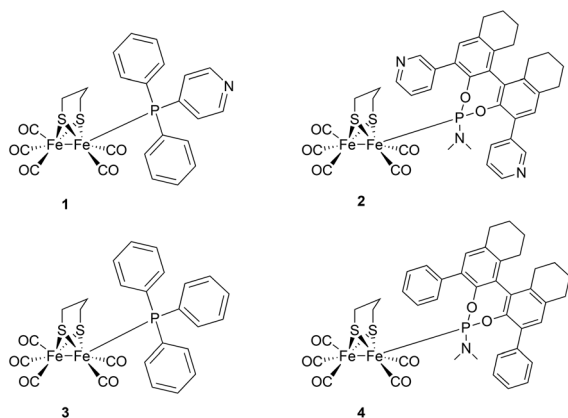


Fig. 2 The novel [FeFe]H<sub>2</sub>ase biomimetic catalyst **2** based on the phosphoramidite ligand appended with two 3-pyridyl groups (*mPyPA*) and the reference complexes **1**, **3** and **4**.

by the properties such ligand could impart onto the diiron core. Phosphoramidites have better  $\pi$ -acceptor properties compared to the related phosphines, likely removing electron density from the diiron core. This would lead to less negative reduction potentials of the complex and, therefore, smaller overpotential for H<sub>2</sub> production. Furthermore, the two pyridyl side groups on the ligand may facilitate the association of macrocyclic chromophores to the metal centre and/or participate in proton transfer.

Complex **2** [Fe<sub>2</sub>( $\mu$ -pdt)(CO)<sub>5</sub>(*mPyPA*)] was synthesised together with the pyridyl-free complexes **3** [Fe<sub>2</sub>( $\mu$ -pdt)(CO)<sub>5</sub>(PPh<sub>3</sub>)] and **4** [Fe<sub>2</sub>( $\mu$ -pdt)(CO)<sub>5</sub>(PhPA)] serving for control experiments (Fig. 2). The syntheses of **2** and **4** involve substitution of one carbonyl ligand in [Fe<sub>2</sub>( $\mu$ -pdt)(CO)<sub>6</sub>] for the phosphoramidite ligand: <sup>31</sup>P NMR spectra as well as MS of the new compounds revealed single CO displacement and phosphoramidite coordination to the Fe centre *via* the phosphorus atom, leaving, in each case, both pyridyl groups on the phosphoramidite free for coordination to the photosensitizer.

The IR spectra show a characteristic  $\nu$ (CO) pattern of [Fe<sub>2</sub>( $\mu$ -pdt)(CO)<sub>5</sub>L] (Table 1) and carbonyl stretching shifted *ca.* 30 cm<sup>-1</sup> to smaller wavenumbers with respect to [Fe<sub>2</sub>( $\mu$ -pdt)(CO)<sub>6</sub>]. Surprisingly, the  $\nu$ (CO) values are very close to those for the pyridylphosphine derivative **1**, demonstrating that the electronic difference between the pyridylphosphine and phosphoramidite ligands is not translated into Fe-to-CO  $\pi$ -backdonation and hence into differences in electron density at the iron core.

Table 1 The IR  $\nu$ (CO) wavenumbers of complexes **1** to **4** in dichloromethane

Complex	$\nu$ (CO) [cm <sup>-1</sup> ]
<b>1</b> (ref. 7)	2048 (s), 1985 (s), 1966 (sh), 1937 (m)
<b>2</b>	2047 (s), 1993 (s), 1975 (s), 1962 (m)
<b>3</b> (ref. 10)	2044 (s), 1984 (s), 1931 (m)
<b>4</b>	2045 (s), 1992 (s), 1973 (m), 1961 (sh)

Table 2 Electrochemical data of compounds **1** to **4** in butyronitrile. For an explanation on electrochemical reaction orders (*n*) and rate constants (*k'*), see text. All potentials are vs. Fc/Fc<sup>+</sup>. Observed rate constant *k*<sub>obs</sub> at 7 mM acetic acid concentration

Complex	<i>E</i> <sub>pc1</sub> [V]	<i>E</i> <sub>pc2</sub> [V]	<i>n</i>	<i>k'</i>	<i>k</i> <sub>obs</sub> [s <sup>-1</sup> ]
<b>1</b>	-1.78	-2.24	1.79	17.8	580
<b>2</b>	-1.88	-2.28	3.58	6.00	6340
<b>3</b>	-1.81	-2.26	2.31	1.44	130
<b>4</b>	-1.90	-2.38	2.85	0.93	240

In line with this observation, cyclic voltammetry shows that **1–4** have their (irreversible) first cathodic waves placed at roughly the same electrode potential (Table 2). The electrocatalytic activity of these complexes towards proton reduction was studied at a static mercury drop electrode by examining the growth of their cathodic waves upon addition of acetic acid under identical experimental conditions (Fig. 3). Again, catalytic waves for all four compounds were found at roughly the same potential (-2.4 V vs. Fc/Fc<sup>+</sup>).§ Adsorption of the pyridine-functionalized complexes to the mercury surface was not observed.¶

Although both cathodic and catalytic wave potentials for all four studied complexes are similar, the current maxima and shapes of the catalytic waves have indicated that there is a remarkable difference in activity. To understand this difference, in-depth analysis was performed on the cyclic voltammograms for each complex. The observed rate constant *k*<sub>obs</sub> has been determined by the method of DuBois and co-workers (eqn (1)),<sup>11</sup> using the ratio between the second cathodic peak current (*i*<sub>pc2</sub>) and the catalytic peak current (*i*<sub>cat</sub>) under the assumption that H<sub>2</sub> formation is irreversible (*E*<sub>r</sub>*C*<sub>i</sub> mechanism). Remarkably, catalytic efficiency is much higher for catalyst precursor **2**, as reflected in the much larger *k*<sub>obs</sub> (~6000 s<sup>-1</sup> at 7 mM acetic acid) compared to **1**, **3** and **4** (Fig. 4). Since all catalysts operate at similar potentials, the effect of differences

§ Cyclic voltammograms of **1** in ref. 7 showed electrocatalytic proton reduction at the potential coinciding with the first cathodic wave. However, these voltammograms were recorded using a glassy carbon working electrode, which gives competing direct reduction, thereby increasing the observed “catalytic” current.<sup>18</sup> Repeating the same experiments using a static mercury drop electrode has revealed that the true catalytic response is in fact not at the first cathodic wave, but shifted more negatively by *ca.* 0.6 V.

¶ It is known that pyridine (and pyridine-functionalized molecules) can adsorb to mercury surfaces.<sup>19</sup> If this were the case for complexes **1** and **2**, their cyclic voltammograms would diverge significantly from those recorded for complexes **3** and **4**, respectively. Namely, the cathodic peaks would be broadened<sup>20</sup> and diffusion-related behaviour would be suppressed. However, we have observed almost identical cyclic voltammograms for **1** and **3**, and **2** and **4** (*cf.* ESI, Fig. S11†) which are in their turn similar to cyclic voltammograms published in literature (on Pt and glassy carbon).<sup>10</sup> Furthermore, we have conducted cyclic voltammetry of complex **2** at different scan rates (0.05 to 5.0 V s<sup>-1</sup>) using both static mercury drop and platinum microdisc working electrodes and found a linear relationship between the cathodic peak current and the square root of the scan rate (*cf.* ESI, Fig. S13 and S14†). Since this behaviour corresponds with the diffusion control of mass transport in the double-layer region of the working electrode in line with the Randles-Sevcik equation, we assume no significant surface adsorption for the major species in the electrolyte solution.



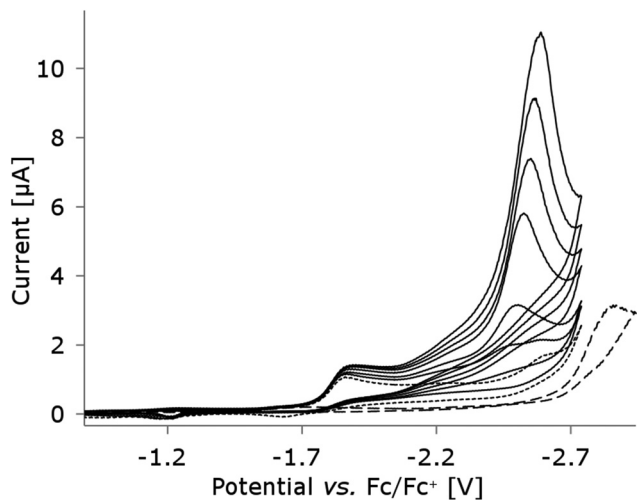


**Fig. 3** Cyclic voltammety of complex 2 (1.0 mM) in butyronitrile containing 0.1 M  $(n\text{Bu})_4\text{NPF}_6$  showing an effect of increasing acetic acid concentration: 0 (dotted), 1, 2, 4, 5, 6, and 7 mM. Conditions: static mercury drop (SMD) working electrode, scan rate  $0.1 \text{ V s}^{-1}$ . The dashed line represents direct (background) proton reduction for 7 mM acetic acid in butyronitrile in the absence of catalyst.

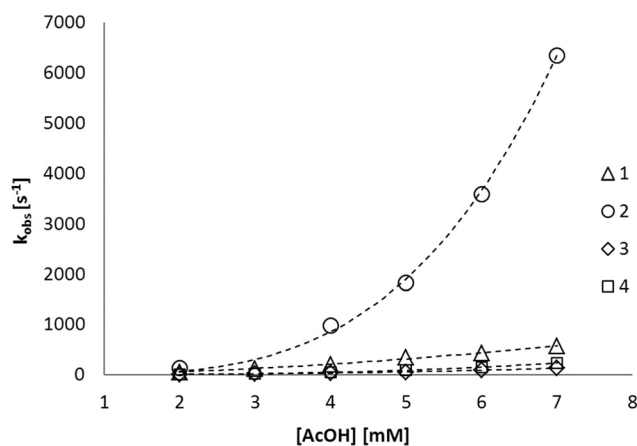


**Fig. 4** Plotted dependence of the rate constant  $k_{\text{obs}}$  on acetic acid concentration for complexes 1 to 4. Dashed lines are curve fits of the form  $y = ax^n$ . For fit parameters,  $R^2$  values and zoomed-in graph ( $k_{\text{obs}} < 600 \text{ s}^{-1}$ ) see the ESI.†

in overpotential on the catalytic rate can be neglected,<sup>12</sup> and therefore the rate increase might well be caused by differences in particular mechanisms of the  $\text{H}_2$  evolution.

$$k_{\text{obs}} = 0.0497 \frac{F\nu}{RT} \left( \frac{i_{\text{cat}}}{i_{\text{p}}} \right) \quad (1)$$

$$\frac{\partial[\text{H}_2]}{\partial t} = k'[\text{H}^+]^n \quad (2)$$

In line with behaviour of the natural system and observations from recent model complexes,<sup>13</sup> it seems eminent that proton preorganization plays a role in accelerating the catalytic reduction. To get more insight into the proton-reactive behaviour, a relation between the rate of the  $\text{H}_2$  formation and acid

concentration was sought by equating  $k_{\text{obs}}$  to  $\partial[\text{H}_2]/\partial t$ . The obtained curve ( $k_{\text{obs}}$  vs.  $[\text{H}^+]$ ) is then characterised by the rate constant  $k'$  and reaction order  $n$  in a pseudo rate equation proportional to the kinetics of the reaction under study. Fitting our data points to a power function (eqn (2)) has yielded values for  $k'$  and  $n$  for each complex under study (Table 2) with  $R^2$  values between 0.993 and 0.999.

The obtained pseudo rate equation for (electro)catalysis takes into account the step(s) just before the rate determining step, including additional protonation equilibria (if any).<sup>14</sup> On this basis a correlation between rate order and constant, and Brønsted basic sites has been found: Phosphine complexes 1 and 3 show a reaction order close to 2, whereas for phosphoramidite complexes 2 and 4,  $n$  has been found close to 3, suggesting additional protonation equilibria. Since phosphoramidites can be protonated on the dimethylamine moiety, proton preorganization might explain the differences in the reaction order. It has been shown for multiple proton reduction catalysts that a proton relay close to the active site can indeed increase their activity, supporting the hypothesis of proton preorganization in the case of the phosphoramidite complexes.<sup>15</sup>

Still, this does not explain why complex 2 is much more active than its phenyl analogue 4. However, it has been found that the pseudo rate constants for phenyl-functionalized 3 and 4 are considerably smaller than those for pyridyl-functionalized 1 and 2. This pyridyl-induced rate increase might be explained by an electronic communication between the ligand and iron core or by stabilisation of the mono-reduced intermediate.<sup>8a,9</sup>

From this analysis, it is believed that for the high electrocatalytic rate observed for 2, both phosphoramidite and pyridyl functionalities are mandatory. The dimethylamino moiety might act as a proton relay, whereas the role of the pyridyl functionality remains unclear. This distinct ligand effect also implies that the active species contains at least one ligand moiety. However, since it is known that  $\text{Fe}_2(\mu\text{-pdt})$  complexes undergo a variety of transformations on one-electron reduction, it is unclear whether the active species is in fact one-electron reduced 2 or one of its secondary reduction products. Although its exact structure remains elusive, the active species formed after reduction of precatalyst 2 shows a much higher electrocatalytic activity than its phosphine analogue.

Complex 2 shows an irreversible one-electron reduction wave, consistent with previously reported mono-substituted pentacarbonyl  $\text{Fe}_2(\mu\text{-pdt})$  complexes.<sup>10</sup> Furthermore, on one-electron reduction, complex 1 has been shown to disproportionate into the parent hexacarbonyl and the disubstituted tetracarbonyl complex.<sup>7</sup> Spectroelectrochemistry (SEC) on 2 shows an identical behaviour (cf. ESI, Fig. S15 to S17†). However, on the short time scale of cyclic voltammety (defined by  $\nu = 100 \text{ mV s}^{-1}$  as opposed to  $2 \text{ mV s}^{-1}$  for SEC), it is reasonable to assume that during catalysis a rather complex chemical mixture is present, consisting of precatalyst 2, one-electron reduced 2<sup>-</sup>, its disproportionation products (the hexacarbonyl and the disubstituted complexes 5, see ESI†), their respective decomposition products (a mixture of  $\text{Fe}_2$  and  $\text{Fe}_4$  clusters with or without bridging CO and thiolate ligands) plus all possible protonated species.



Having established that compound **2** is a precursor of a good proton reduction catalyst, we analysed its photocatalytic behaviour when combined with zinc tetraphenylporphyrin (ZnTPP). Comparison of the catalytic potential of **2** (roughly  $-2.5$  V vs.  $\text{Fc}/\text{Fc}^+$ ) with the second reduction potential of the porphyrin belonging to its singlet excited state ( $-1.75$  V vs.  $\text{Fc}/\text{Fc}^+$ ) shows that the quenching of ZnTPP\* by **2** is thermodynamically uphill, making photocatalysis for this system unfeasible.\*\*

Despite this, we still trust that the overall supramolecular strategy is worth investigating, since using *e.g.* aromatic dithiolates instead of the propanedithiolate bridge in the studied complexes (Fig. 2), the catalytic potential may well be shifted towards a range well-accessible for ZnTPP.<sup>16</sup> Therefore, we studied the supramolecular assemblies of the pyridyl-functionalised phosphoramidite ligand and its diiron pentacarbonyl complex with ZnTPP. First, the binding of ZnTPP to the pyridyl groups at the *m*PyPA ligand in complex **2** was determined by means of UV-Vis titration (ESI†). Free *m*PyPA binds two ZnTPP macrocycles with equal association constants ( $2K_{a1} = 0.5K_{a2} = 8.6 \times 10^3 \text{ M}^{-1}$ ), which also applies for the assembly with complex **2** ( $2K_{a1} = 0.5K_{a2} = 9.5 \times 10^3 \text{ M}^{-1}$ ). These data suggest that the interaction is a regular pyridyl-ZnTPP association (typical value in dichloromethane  $6.9 \times 10^3 \text{ M}^{-1}$ ).<sup>17</sup>

## Conclusions

In summary, we report the synthesis and properties of a novel 3-pyridylphosphoramidite-ligated [FeFe]<sub>2</sub>H<sub>2</sub>ase model. Compared to the previously reported 4-pyridylphosphine analogue, complex **2** is much more active in the reduction of protons at a similar overpotential, which could be attributed to the dimethylamine moiety acting as a proton relay. The pyridyl functionality on the phosphoramidite ligand also plays a crucial role in accelerating proton reduction, although its exact function has not yet been elucidated.

Furthermore, the supramolecular host-guest-host assembly ZnTPP-**2**-ZnTPP forms in non-coordinating solvents without any cooperative behaviour. However, it was shown that complex **2** neither quenches the excited state of the chromophore, nor reaches the thermodynamic potential needed for photocatalysis. Further matching of redox levels of the catalyst core and the associated chromophore will show if photo-driven hydrogen formation is viable using the same phosphoramidite ligand. One way to achieve this goal would be the replacement of the propanedithiolate bridge by an aromatic bridge, effectively shifting the cathodic potential to less negative values.<sup>5,16</sup>

\*\*A luminescence titration was carried out, monitoring the light emission of ZnTPP in the presence of an increasing amount of **2**. Instead of static quenching by electron transfer, a red shift of the emission was observed which can be assigned to emission of the assembly **2**-ZnTPP. Preliminary photocatalytic experiments using this system led, *in all cases*, to decomposition of the catalyst with evolution of 0.5 equivalents of H<sub>2</sub> with respect to the catalyst.

## Acknowledgements

This work has been supported (S.D. and P.L.) by the Netherlands' Organization for Scientific Research (NWO-CW, ECHO grant 700.57.042) and the BioSolar Cells program (R.B.). We acknowledge Dr A. M. Kluwer (InCatT BV) for fruitful discussions, and Dr R. Bellini (UvA) and Drs Bart van den Bosch (UvA) for ligand synthesis.

## Notes and references

- (a) N. Armaroli and V. Balzani, *ChemSusChem*, 2011, **4**, 21; (b) N. S. Lewis and D. G. Nocera, *Proc. Natl. Acad. Sci. U. S. A.*, 2006, **103**, 15729; (c) A. J. Esswein and D. G. Nocera, *Chem. Rev.*, 2007, **107**, 4022.
- (a) M. P. McLaughlin, T. M. McCormick, R. Eisenberg and P. L. Holland, *Chem. Commun.*, 2011, **47**, 7989; (b) T. S. Teets and D. G. Nocera, *Chem. Commun.*, 2011, **47**, 9268; (c) M. L. Helm, M. P. Stewart, R. M. Bullock, M. Rakowski Dubois and D. L. Dubois, *Science*, 2011, **333**, 863; (d) P.-A. Jacques, V. Artero, J. Pecaut and M. Fontecave, *Proc. Natl. Acad. Sci. U. S. A.*, 2009, **106**, 20627; (e) V. Artero and M. Fontecave, *Coord. Chem. Rev.*, 2005, **249**, 1518; (f) X. Zong, Y. Na, F. Wen, G. Ma, J. Yang, D. Wang, Y. Ma, M. Wang, L. Sun and C. Li, *Chem. Commun.*, 2009, 4536.
- R. K. Thauer, *Eur. J. Inorg. Chem.*, 2011, 919.
- (a) J.-F. Capon, F. Gloaguen, F. Y. Pétillon, P. Schollhammer and J. Talarmin, *Coord. Chem. Rev.*, 2009, **253**, 1476; (b) J. C. Fontecilla-Camps, A. Volbeda, C. Cavazza and Y. Nicolet, *Chem. Rev.*, 2007, **107**, 4273; (c) M. Y. Darensbourg, E. J. Lyon and J. J. Smee, *Proc. Natl. Acad. Sci. U. S. A.*, 2003, **100**, 3683; (d) M. Y. Darensbourg, E. J. Lyon and J. J. Smee, *Coord. Chem. Rev.*, 2000, **206**, 533; (e) F. Gloaguen and T. B. Rauchfuss, *Chem. Soc. Rev.*, 2009, **38**, 100; (f) M. Schmidt, S. M. Contakes and T. B. Rauchfuss, *J. Am. Chem. Soc.*, 1999, **121**, 9736.
- G. A. N. Felton, C. A. Mebi, B. J. Petro, A. K. Vannucci, D. H. Evans, R. S. Glass and D. L. Lichtenberger, *J. Organomet. Chem.*, 2009, **694**, 2681.
- (a) L.-C. Song, M.-Y. Tang, S.-Z. Mei, J.-H. Huang and Q.-M. Hu, *Organometallics*, 2007, **26**, 1575; (b) M. Wang, Y. Na, M. Gorlov and L. Sun, *Dalton Trans.*, 2009, 6458; (c) F. Wang, W. G. Wang, X. J. Wang, H. Y. Wang, C.-H. Tung and L. Z. Wu, *Angew. Chem., Int. Ed.*, 2011, **50**, 3193; (d) R. Lomoth and S. Ott, *Dalton Trans.*, 2009, 9952; (e) M. Wang, L. Chen, X. Lia and L. Sun, *Dalton Trans.*, 2011, **40**, 12793.
- A. M. Kluwer, R. Kapre, F. Hartl, M. Lutz, A. L. Spek, A. M. Brouwer, P. W. N. M. van Leeuwen and J. N. H. Reek, *Proc. Natl. Acad. Sci. U. S. A.*, 2009, **106**, 10460.
- For template-ligand approach in other reactions see: (a) V. F. Slagt, M. Röder, P. C. J. Kamer, P. W. N. M. van Leeuwen and J. N. H. Reek, *J. Am. Chem. Soc.*, 2004, **126**, 4056; (b) M. Kuil, P. E. Goudriaan, P. W. N. M. van Leeuwen



- and J. N. H. Reek, *Chem. Commun.*, 2006, 4679; (c) M. Kuil, P. E. Goudriaan, A. W. Kleij, D. M. Tooke, A. L. Spek, P. W. N. M. van Leeuwen and J. N. H. Reek, *Dalton Trans.*, 2007, 2311; (d) A. W. Kleij, M. Lutz, A. L. Spek, P. W. N. M. van Leeuwen and J. N. H. Reek, *Chem. Commun.*, 2005, 3661; (e) A. W. Kleij, D. M. Tooke, A. L. Spek and J. N. H. Reek, *Eur. J. Inorg. Chem.*, 2005, 4626; (f) A. W. Kleij and J. N. H. Reek, *Chem. – Eur. J.*, 2006, **12**, 4218; (g) T. Gadzikwa, R. Bellini, H. L. Dekker and J. N. H. Reek, *J. Am. Chem. Soc.*, 2012, **134**, 2860.
- 9 R. Bellini, S. H. Chikkali, G. Berthon-Gelloz and J. N. H. Reek, *Angew. Chem., Int. Ed.*, 2011, **50**, 7342.
- 10 P. Li, M. Wang, C. He, G. Li, X. Liu, C. Chen, B. Åkermark and L. Sun, *Eur. J. Inorg. Chem.*, 2005, 2506.
- 11 A. D. Wilson, R. H. Newell, M. J. McNevin, J. T. Muckerman, M. Rakowski DuBois and D. L. DuBois, *J. Am. Chem. Soc.*, 2006, **128**, 358.
- 12 C. Costentin, S. Drouet, M. Robert and J.-M. Savéant, *J. Am. Chem. Soc.*, 2012, **134**, 11235.
- 13 D. Schilter and T. B. Rauchfuss, *Angew. Chem., Int. Ed.*, 2013, **51**, 13518.
- 14 D. H. Pool and D. L. DuBois, *J. Organomet. Chem.*, 2009, **694**, 2858.
- 15 U.-P. Apfel, *Models for the Active Site of the [FeFe]-Hydrogenase*, Ph.D. Thesis, Friedrich-Schiller-Universität Jena, Jena (D), 2010, pp. 22–25.
- 16 L. Schwartz, P. S. Singh, L. Eriksson, R. Lomoth and S. Ott, *C. R. Chim.*, 2008, **11**, 875.
- 17 A. Satake and Y. Kobuke, *Tetrahedron*, 2005, **61**, 13.
- 18 G. A. N. Felton, R. S. Glass, D. L. Lichtenberger and D. H. Evans, *Inorg. Chem.*, 2006, **45**, 9181.
- 19 L. D. Klyukina and B. B. Damaskin, *Bull. Acad. Sci. USSR*, 1963, **12**, 931.
- 20 H. Gerischer and D. A. Scherson, *J. Electroanal. Chem. Interfacial Electrochem.*, 1985, **188**, 33.

